Excitonic transitions and exchange splitting in Si quantum dots

F. A. Reboredo, A. Franceschetti, and A. Zunger

Citation: Applied Physics Letters **75**, 2972 (1999); doi: 10.1063/1.125205
View online: http://dx.doi.org/10.1063/1.125205
View Table of Contents: http://scitation.aip.org/content/aip/journal/apl/75/19?ver=pdfcov
Published by the AIP Publishing

Excitonic transitions and exchange splitting in Si quantum dots

F. A. Reboredo,[a] A. Franceschetti, and A. Zunger
National Renewable Energy Laboratory, Golden, Colorado 80401

(Received 7 June 1999; accepted for publication 13 September 1999)

In a quantum dot made of an indirect gap material such as Si, the electron–hole Coulomb interaction alone can give rise to ''dark'' excitons even in the absence of exchange interaction. We present the predicted excitonic spectra for hydrogen-passivated Si dots and find very good agreement with the recent experiment of Wolkin, Jorne, Fauchet, Allan, and Delerue [Phys. Rev. Lett. **82**, 197 (1999)]. The calculated splitting between dark and bright excitons, arising from Coulomb and exchange interactions, agrees very well with the optical data of Calcott, Nash, Canham, Kane, and Brumhead [J. Phys Condens. Matter **5**, L91 (1993)]. © *1999 American Institute of Physics.* [S0003-6951(99)04845-7]

Excitons represent electron–hole pairs bound by their Coulomb attraction and by the parallel-spin-exchange interaction. In quantum dots made of direct-gap materials (CdSe, InAs, or InP) the Coulomb attraction merely shifts uniformly the energy of the lowest excitonic state, while the exchange interaction splits the excitonic line into a low-lying forbidden (''dark'') state and a higher-energy-allowed (''bright'') state. This gives rise to an absorption versus emission Stokes shift,[1] which is used to assess experimentally the exchange splitting. In quantum dots made of indirect-gap materials (e.g., Si), on the other hand, already the Coulomb interaction splits the exciton into spatially allowed and spatially forbidden excitons. Exchange interaction leads to further spin splitting. Using a pseudopotential description of hydrogen-passivated Si dots, we predict here the excitonic spectra, including (i) excitonic gap versus size, (ii) Coulomb splittings, and (iii) exchange splittings of Si dots. We compare the excitonic gaps with the recent photoluminescence (PL) data of Wolkin *et al.*,[2] and the exchange splitting with the optical data of Calcott *et al.*[3] We find excellent agreement, and provide the fine-structure excitonic multiplet spectra as prediction for future, high-resolution experimental spectroscopic studies.

We consider approximately spherical silicon crystallites centered around a Si atom. The dots thus have T_d point-group symmetry. All Si atoms are assumed to be located at their ideal bulk positions. The surface atoms with three dangling bonds are removed, while those with one or two dangling bonds are passivated with hydrogen atoms, as described in Refs. 4 and 5. The passivated dots are then surrounded by vacuum and placed in a large supercell that is repeated periodically. Having created an (artificially) periodic structure, we can calculate its electronic structure via ordinary $H\psi=\varepsilon\psi$ ''band-structure'' methods applied to the supercell, where the Hamiltonian is given by[5]

$$H=-\frac{\hbar^2}{2m}\nabla^2+\sum_{\mathbf{R}_{Si}} v_{\mathrm{Si}}(\mathbf{r}-\mathbf{R}_{\mathrm{Si}})+\sum_{\mathbf{R}_{\mathrm{H}}} v_{\mathrm{H}}(\mathbf{r}-\mathbf{R}_{\mathrm{H}}), \tag{1}$$

where m is the free-electron mass while v_{Si} and v_{H} are the atomic local empirical pseudopotentials[4,5] of Si and H. v_{Si} was fitted[5] to obtain the bulk band structure at high symmetry points, the effective masses, and the surface work function while v_{H} was fitted[4,5] to obtain the surface local density of states of the three primary [(100), (110), and (111)] H-covered Si films. Effective mass or $\mathbf{k}\cdot\mathbf{p}$ approximations are thus avoided.

We expand the wave functions $\psi(\mathbf{r})$ via a plane-wave basis set and diagonalize the Hamiltonian of Eq. (1) using the folded spectrum method.[5] From the solutions of this single-particle problem we construct a set of single-substitution Slater determinants $\{\Phi_{e,h}\}$, obtained from the ground-state Slater determinant by promoting an electron from the (occupied) valence state ψ_h of energy ε_h to the (unoccupied) conduction state ψ_e of energy ε_e. The exciton wave functions $\Psi^{(\alpha)}$ are expanded in terms of this determinantal basis set:[1,6]

$$\Psi^{(\alpha)}=\sum_{e=1}^{Ne}\sum_{h=1}^{N_h} C_{h,e}^{(\alpha)}\Phi_{h,e}, \tag{2}$$

where N_h and N_e denote the number of hole and electron states included in the expansion of the exciton wave functions. The matrix elements of the many-particle Hamiltonian $\mathcal{H}$ in the basis set $\{\Phi_{h,e}\}$ are calculated as

$$\begin{aligned}\mathcal{H}_{he,h'e'}&\equiv\langle\Phi_{he}|\mathcal{H}|\Phi_{h'e'}\rangle\\&=(\varepsilon_e-\varepsilon_h)\delta_{h,h'}\delta_{e,e'}-J_{he,h'e'}+K_{he,h'e'},\end{aligned} \tag{3}$$

where J and K are the electron–hole Coulomb and exchange integrals, respectively,

$$J_{he,h'e'}=e^2\sum_{\sigma_1,\sigma_2}\int\int\frac{\psi_{h'}^*(\mathbf{r}_1,\sigma_1)\psi_e^*(\mathbf{r}_2,\sigma_2)\psi_h(\mathbf{r}_1,\sigma_1)\psi_{e'}(\mathbf{r}_2,\sigma_2)}{\overline{\epsilon}(|\mathbf{r}_1-\mathbf{r}_2|,R)|\mathbf{r}_1-\mathbf{r}_2|}d\mathbf{r}_1 d\mathbf{r}_2, \tag{4}$$

[a]Electronic mail: frebored@nrel.gov

$$K_{he,h'e'}=e^2\sum_{\sigma_1,\sigma_2}\int\int\frac{\psi_{h'}^*(\mathbf{r}_1,\sigma_1)\psi_e^*(\mathbf{r}_2,\sigma_2)\psi_{e'}(\mathbf{r}_1,\sigma_1)\psi_h(\mathbf{r}_2,\sigma_2)}{\overline{\epsilon}(|\mathbf{r}_1-\mathbf{r}_2|,R)|\mathbf{r}_1-\mathbf{r}_2|}d\mathbf{r}_1d\mathbf{r}_2. \quad (5)$$

The electron–hole Coulomb and exchange integrals of Eqs. (4) and (5) use a screening function $\overline{\epsilon}(\mathbf{r}_1,\mathbf{r}_2,R)$, which depends on the interparticle distance $|r_1-r_2|$ and on the quantum dot radius R. We use the model of Ref. 1 for this screening function. The same model was used to obtain the excitonic spectrum of free-standing InP (Refs. 6 and 7) and CdSe (Refs. 6 and 8) dots.

Figure 1 shows how the various physical factors act to define the excitonic manifold of a 1123 atom Si dot. In this dot, the valence-band maximum and the conduction-band minimum (CBM) both have t_2 symmetry. Thus, the exciton must contain $t_2\times t_2=T_1+T_2+E+A_1$ states. The degeneracies (including spin) are 12, 12, 8, and 4, respectively. In the absence of either Coulomb (J) and exchange (K) interactions [Fig. 1(a)], the exciton is thus 36-fold degenerate. Introduction of Coulomb effects [Fig. 1(b)] shifts and splits the exciton in four states, T_1, T_2, E, and A_1. Only T_2 is optically allowed. The lowest-energy state has A_1 symmetry and is optically forbidden (''dark''). Introduction of exchange effects [Fig. 1(c)] splits each of the four states into a higher-energy singlet, and a lower-energy triplet. Thus, the low-energy $^3A_1$, ^3E, and $^3T_1$ triplet states are both spatially and spin forbidden, the next triplet state $^3T_2$ is forbidden only spin-wise, while the $^1T_1$, $^1A_1$, and ^1E singlet states are only spatially forbidden. Only the $^1T_2$ singlet state is allowed. The dark versus bright splitting is shown in Fig. 2 where we see that it ranges between 0 and 30 meV, has a size scaling of $R^{-2.51}$, and agrees very well with the optical splitting measured by Calcott *et al.* Their thermal data are different from their optical data. Our results lie below the theoretical calculations of Leung and Whaley[9] and above the calculations of Martin *et al.*[10] Introduction of correlation effects via mixing of configurations in Eq. (3) leads to a stabilizing downward shift of all multiplets [Fig. 1(d)]. This latter result constitutes a prediction for the excitonic fine structure of Si quantum dots, to be tested experimentally in the future.

Figure 3 shows the calculated excitonic gap (corresponding to the lowest-energy-allowed exciton) as a function of the dot radius, comparing the results with the experimental data of Wolkin *et al.*[2] Their porous silicon samples were prepared by electrochemical etching followed by photoassisted stain etching. Special care was taken to avoid exposure of the samples to air. The etching process passivates the surface of porous silicon with hydrogen. Wolkin *et al.*[2] measured the PL decay time and the maximum PL energy of each sample as a function of the crystallite size. Figure 3 shows an excellent agreement between theory and experiment for samples that have not been exposed to air. The recent quasiparticle calculation of Ögüt, Chelikowsky, and Louie[11] (shown in Fig. 3 as open triangles) does not agree with experiment as well. The reason for this difference[12] is that instead of equating the excitonic energy with $\varepsilon^{\mathrm{opt}}=\varepsilon_g-J$ (where ε_g is the single-particle energy), Ögüt, Chelikowsky, and Louie[11] use the expression $\varepsilon^{\mathrm{qp}}=[E(N-1)-E(N)]-[E(N)-E(N+1)]-J$. Here, $E(N)$ is the total energy of a dot with N electrons and thus includes polarization effects. However, an additional polarization term is ignored in their calculation of the Coulomb interaction J. Addition of this polarization term to their $\varepsilon^{\mathrm{qp}}$ gives a net result of ε_g-J.

It is interesting to note that whereas simple theories predict that the single-particle band gap scales with size as $\varepsilon_g\sim R^{-2}$ (effective mass theory) and the Coulomb energy scales as $J\sim R^{-1}$, in the more complete pseudopotential calculation $\varepsilon_g\sim R^{-1.2}$ while J (screened with a position-dependent and size-dependent dielectric function) scales as $J\sim R^{-1.5}$. This scaling comes form two factors: (a) the

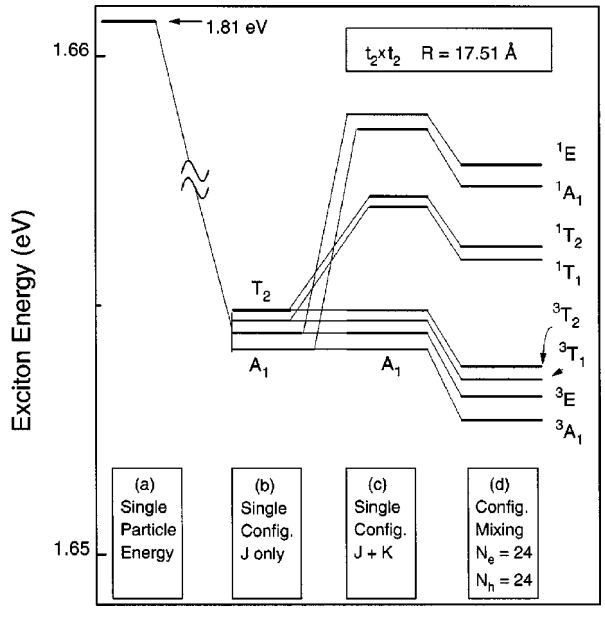

FIG. 1. Exciton energies of a 1123 Si atom dot ($R=17.51$ Å) calculated under different approximations for a $t_2\times t_2$ configuration, indicated in the boxed items (a)–(d).

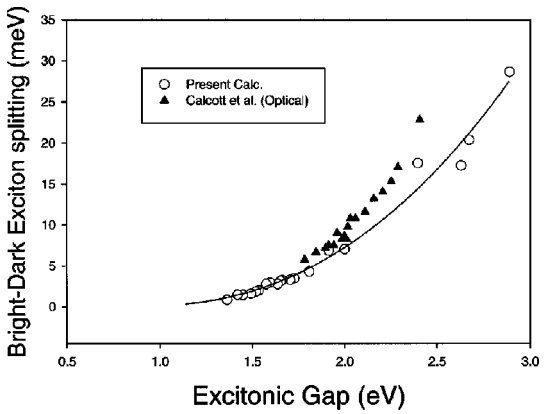

FIG. 2. Energy splitting between the lowest-energy bright exciton and the lowest-energy dark exciton as a function of the dark exciton energy. Circles correspond to the present calculations; the solid continuous line is a guide to the eye. Up triangles correspond to the optical onset measurements of Calcott *et al.* (Ref. 3).

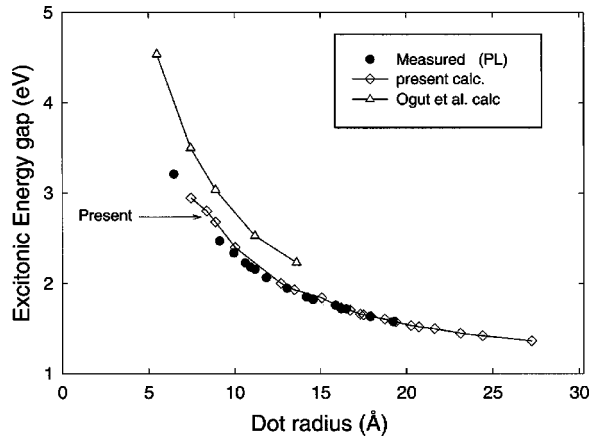

FIG. 3. Comparison between the lowest excitonic gap obtained with different theories and experiments. Full circles correspond to the experimental results of Wolkin *et al.* (Ref. 2), open diamonds to the present pseudopotential calculation, and triangles to the quasiparticle calculations of Ögüt, Chelikowsky, and Louie (Ref. 11).

pseudopotential wave functions are different from envelope functions, and (b) the dielectric screening $\epsilon(r,R)$ entering in J depends on the size R. For silicon dots effect (b) is more important than (a), as seen by the fact that using a size-dependent screening with effective mass wave functions gives $J \sim R^{-1.53}$. Thus, while simple theory suggests that Coulomb effects tend to become less important as size diminishes, a more accurate calculation shows that Coulomb effects are more important than quantum-confinement effects at small sizes.

In summary, we have found that the electron–hole Coulomb interactions are very important in determining the symmetry of excitons in quantum dots made of a bulk indirect-gap material. In particular, (i) direct Coulomb interactions are able to split the energies of excitons which are degenerate in the single-particle approximation. (ii) When the symmetry of the CBM is t_2, the direct Coulomb interaction lowers the energy of a dark exciton below the optically active ones. (iii) When the symmetry of the CBM is not t_2, the lower-energy excitons have T_2 symmetry. (iv) Exchange corrections raise the energy of singlet states. (v) We found that our calculated dark–bright excitonic splitting agrees very well with the experimental optical data of Calcott *et al.*[3] Finally, (vi) in contradiction with simple textbook arguments, we have found that the relevance of the Coulomb direct interaction, exchange interaction, and correlation effects increase as compared to the single-particle energy splittings for smaller dots.

The authors would like to thank to Lin-Wang Wang for supplying some of the programs used in this work and for stimulating discussions. This work was supported by BES under Contract No. DE-AC36-98-GO10337.

[1] A. Franceschetti, L. W. Wang, H. Fu, and A. Zunger, Phys. Rev. B **58**, R13367 (1998), and references therein.
[2] M. V. Wolkin, J. Jorne, P. M. Fauchet, G. Allan, and C. Delerue, Phys. Rev. Lett. **82**, 197 (1999).
[3] P. D. Calcott, K. J. Nash, L. T. Canham, M. J. Kane, and D. Brumhead, J. Phys.: Condens. Matter **5**, L91 (1993).
[4] S. B. Zhang, C. Y. Yeh, and A. Zunger, Phys. Rev. B **48**, 11204 (1993).
[5] L. W. Wang and A. Zunger, in *Semiconductor Nanostructures,* edited by P. V. Kamat and D. Meisel (Elsevier Science, New York, 1996), Vol. 103, p. 161.
[6] A. Franceschetti, H. Fu, L. W. Wang, and A. Zunger, Phys. Rev. B **60**, 1819 (1999).
[7] H. Fu and A. Zunger, Phys. Rev. B **57**, R15064 (1998).
[8] L. W. Wang and A. Zunger, Phys. Rev. B **53**, 9579 (1996).
[9] K. Leung and K. B Whaley, Phys. Rev. B **56**, 7455 (1997).
[10] E. Martin, C. Delerue, G. Allan, and M. Lannoo, Phys. Rev. B **50**, 18258 (1994).
[11] S. Ögüt, J. Chelikowsky, and S. Louie, Phys. Rev. Lett. **79**, 1770 (1997).
[12] A. Franceschetti, L.-W. Wang, and A. Zunger, Phys. Rev. Lett. **83**, 1269 (1999).